

School of Mechanical, Aerospace & Automotive Engineering
Faculty of Engineering, Environment and Computing
Coventry, United Kingdom



Coventry
University

6063MAA Coursework 2

Written By:

Ravi Chaudhary, 10947986

Agris Gavars, 10308903

Emils Pless, 10326491

Jenner Romero Leon, 9699487

Table of contents

Abstract.....	4
Design modeller	4
Meshing techniques.....	5
Assumptions.....	6
Model setup.....	6
Mesh Independence study.....	7
Results.....	9
Convergence criteria.....	12
Pressure gradient.....	12
Velocity profile.....	13
Turbulence profile.....	14
Temperature profile.....	15
Discussion.....	16
Conclusion.....	17
Bibliography	18
Appendix	19

List of figures

Figure 1: 3D model geometry	4
Figure 2: Final mesh	5
Figure 3: Closer view of the 3D mesh	6
Figure 4: Skewness mesh metrics and orthogonal quality mesh metrics spectrums	6
Figure 5: Hot outlet temperature against number of elements	8
Figure 6: Cold outlet temperature against number of elements	8
Figure 7: Experimental, 2D and 3D results for experiment 2	11
Figure 8: Experimental, 2D and 3D results for experiment 1	11
Figure 9: Residual convergence graph of a 3D model at a heater temperature of 56.7 °C	12
Figure 10: Isometric view of the change in pressure	13
Figure 11: Isometric view of the velocity profile	14
Figure 12: Turbulence profile	15
Figure 13: Temperature profile	16

List of tables

Table 1: Dimensions of the 3D model	5
Table 2: Setup used to run the mathematical model.	7
Table 3: Mesh independence study of a 3D model at a heater temperature of 55.6°C	7
Table 4: 3D simulation results for experiment 1	10
Table 5: 3D simulation results for experiment 2	10

Abstract

This report expands on coursework 1 and covers the development of a 3D model of the same concentric tube heat exchanger. The aim of this report is to compare the performance of a 3D model simulation to a 2D simulation model in reference to the experimentally obtained results. This report describes the design, meshing and model set-up of a 3D model. The results from the simulation are then compared to the experimental results and the results of the 2D simulation. The advantages and disadvantages, sources of errors and areas of improvement are discussed and summarised.

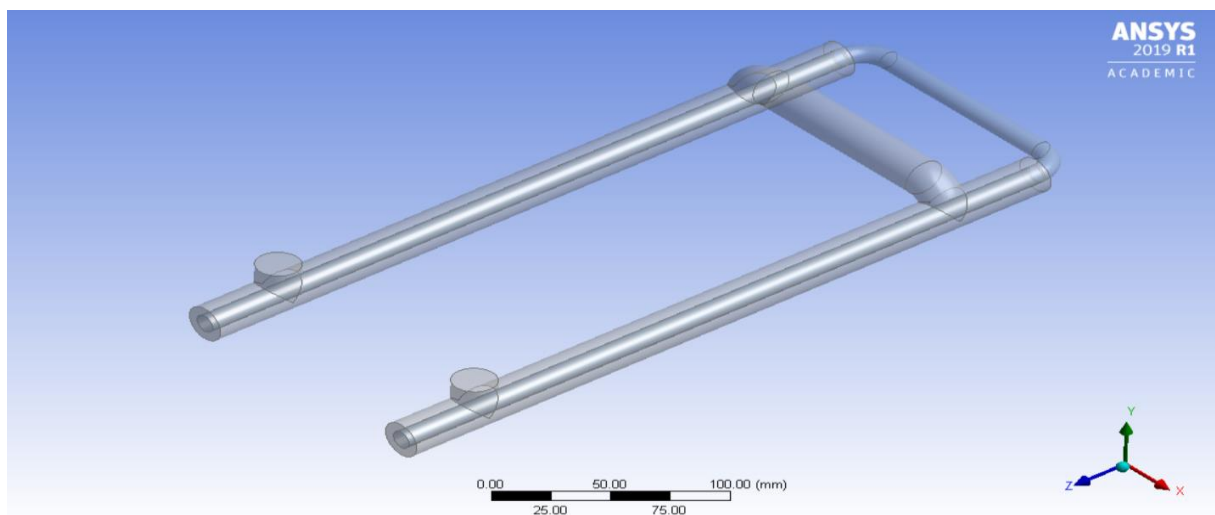
Design modeller

The 3D design of the heat exchanger pipe was created using the Ansys fluent software. The geometry was created using the specification of the heat exchanger TD360a. Some of the dimensions are self-created as some of the required dimensions are not provided in TD360a specification, for instance, the corner radius of the pipe.

The mathematical model was created to understand and observe the heat transfer between the two fluids. Therefore, the quality of mesh is a key factor to obtain accuracy in the results and has an impact on three key areas: rate of convergence, iterations, and result accuracy.

Figure 1 shows the created model.

Figure 1: 3D model geometry



Note. Own creation.

One side of the tube was designed, and the other side was mirrored about the ZY axis, which was possible due to the symmetrical shape of the heat exchanger. The dimensions used to create the 3D model are shown in table 1.

The edge size in the outer pipe was defined with a number of divisions of 70 due to its larger diameter and length. The edge size in the inner pipe was defined with a division number of 50. The other mesh selected was the automatic mesh and the tetrahedrons mesh. The default mesh size was varied between 10mm to 1.5mm for mesh independence check.

Table 1: Dimensions of the 3D model

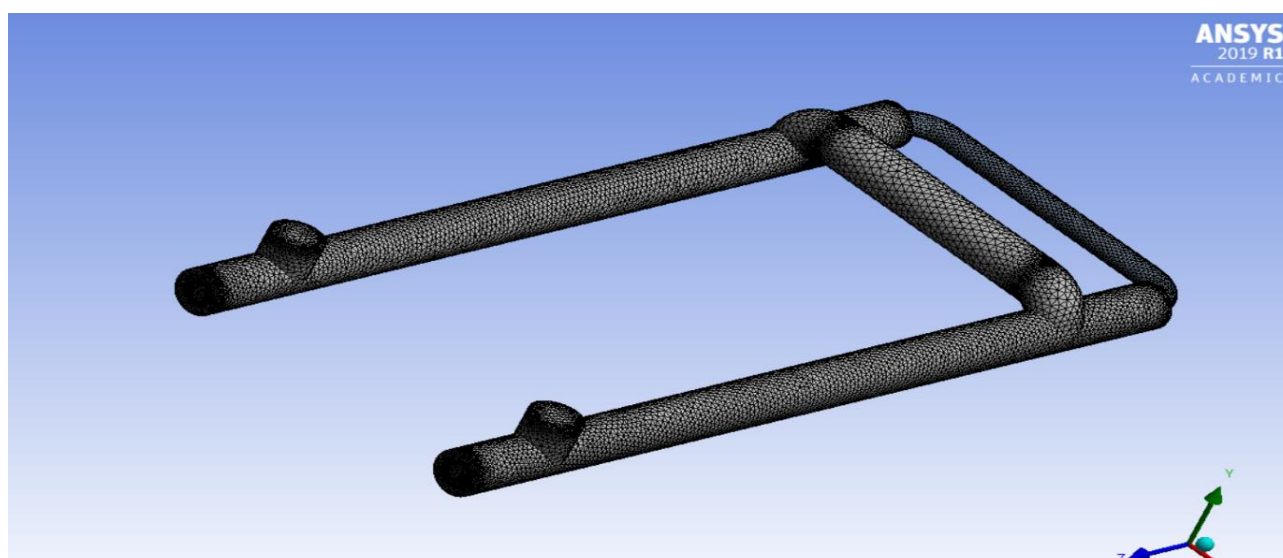
	Inner tube (mm)	Outer tube (mm)
Length of tube	350(*2)	350(*2)
Tube diameter	10	20
Thickness	1	5
Corner radius	14	14

Note. Own creation.

Meshing techniques

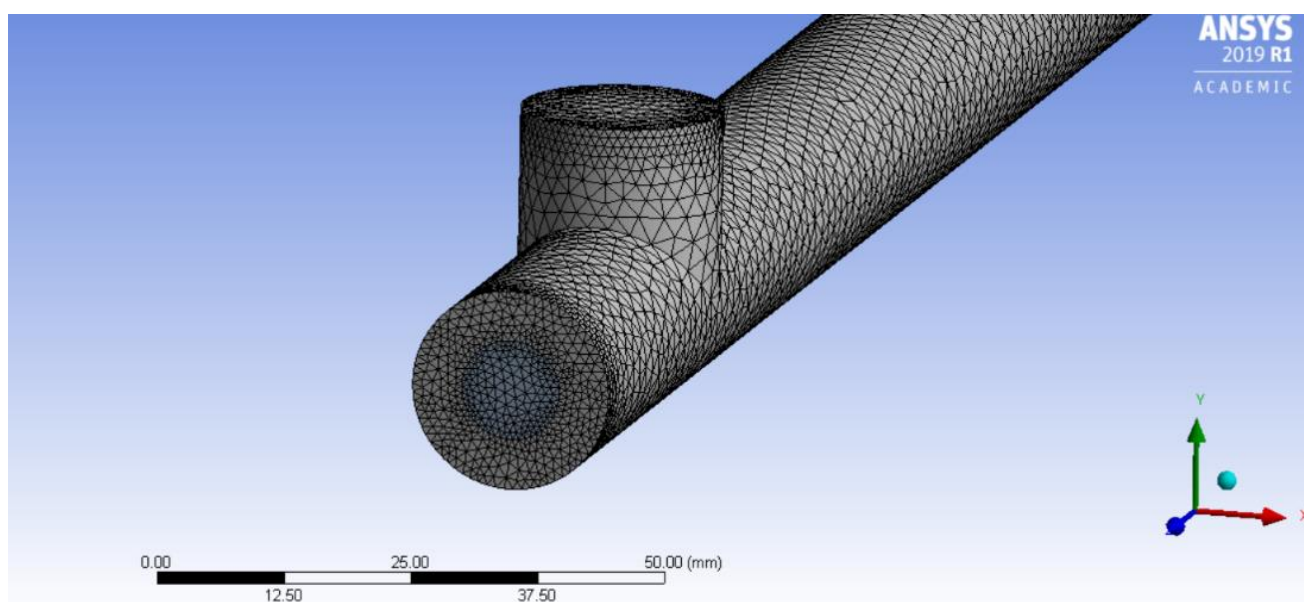
In the mesh section, the parts of the model were specified to give it a physical meaning. A default mesh was generated and later the face sizing, edge sizing, automatic method as well as tetrahedral geometry mesh were used to consolidate the mesh. The edge sizing was used to specify a local growth rate for any cells that move away from this edge and to make the element size finer at the edge of inlet and outlet of the inner and outer pipe. Similarly, the face meshing was used to control the mesh size on the inlet and outlet faces of the inner pipe. The automatic method and the tetrahedral geometry are used to generate an unstructured and a structured mesh in the inner and outer pipe domain and the smoothing was set to high to improve the quality of tetrahedral meshes. The meshes of different element sizes can be found in appendix. Figure 2 features the final mesh with an element size of 4×10^{-3} m. Figure 3 provides a closer view of one end of the heat exchanger.

Figure 2: Final mesh



Note. Own creation.

Figure 3: Closer view of the 3D mesh



Note. Own creation.

Figure 4 provides an illustration of the desired mesh qualities. The created mesh has a skewness of 0.77599 and an orthogonal quality of 0.22401. Both values are considered very good quality.

Figure 4: Skewness mesh metrics and orthogonal quality mesh metrics spectrums

Skewness mesh metrics spectrum

Excellent	Very good	Good	Acceptable	Bad	Unacceptable
0-0.25	0.25-0.50	0.50-0.80	0.80-0.94	0.95-0.97	0.98-1.00

Orthogonal Quality mesh metrics spectrum

Unacceptable	Bad	Acceptable	Good	Very good	Excellent
0-0.001	0.001-0.14	0.15-0.20	0.20-0.69	0.70-0.95	0.95-1.00

Note. (Tips., 2021).

Assumptions

The following assumptions were made to carry out the mathematical model:

1. The flow is full developed and at each temperature change, the system was given time to reach a steady state.
2. Insulated outer pipe walls: no heat loss condition.
3. Uniform hot and cold uniform temperatures.
4. No back flow condition.

Model setup

Table 2 shows the setup used to derive the results using mathematical model. The boundary condition section values were specifically considered for the changes in temperature experiments performed in the lab.

Table 2: Setup used to run the mathematical model.

Setup condition	Chosen option
Energy equation	On
Viscous	K-epsilon Realizable Enhanced wall treatment
Materials- Fluids Inner Pipe (solid) Outer Pipe (solid)	Water-liquid (H ₂ O) Stainless Steel Acrylic (PMMA)
Cell zone conditions- Cold domain Hot domain	Coldwater liquid Hot water liquid
Boundary conditions- Cold Inlet temperature Mass Flow Inlet (cold) Hot Inlet Temperature Mass Flow Outlet (Hot) Outer Pipe (acrylic wall) Thickness of Inner wall (Stainless Steel)	21.4-degree Celsius 0.0198 kg/s 51.4-degree Celsius 0.0117 kg/s Insulated (heat flux set to 0) 1mm
Monitor- Residual	All the check convergence absolute criteria set to 1×10^{-6} store Iterations- 1000
Surface Integrals	Hot Inlet, hot outlet, cold inlet, cold outlet

Note. Own creation.

In the viscous setup condition, k-epsilon was selected as the flow in the experiment was determined to be transient. The k-epsilon model is composed of two equations to solve conservation equations. It also resolves two transport equations (PDEs), which consider historical effects such as turbulent energy convection and diffusion. Similarly, the realizable model was used over the standard within the k-epsilon because it contains a unique expression for the turbulent viscosity (Simscale, n.d.). The enhanced wall treatment is feasible to replicate a transition occurrence, which is typically referred to as the two-layer zonal model. The screenshot of setups could be found in the appendix.

Mesh Independence study

Mesh independence was investigated for a particular model by testing different mesh methods and mesh size to produce a mesh of higher quality. The aspect ratio, skewness, and orthogonal quality of the mesh were all taken into consideration and the simulation was performed. The outlet temperature values were unaffected by changes in element size after a certain threshold with a good-quality mesh, as shown in table 3.

Table 3: Mesh independence study of a 3D model at a heater temperature of 55.6°C

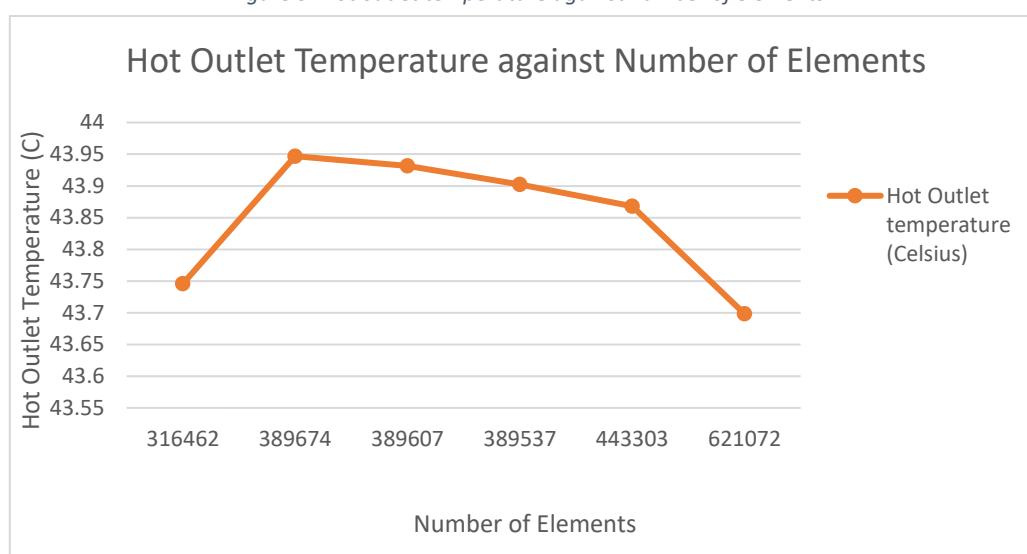
Element size (m)	Number of Elements	Hot Outlet temperature (Celsius)	Cold Outlet temperature (Celsius)
12.4×10^{-2}	316462	43.746024	27.081179
10×10^{-3}	389674	43.946892	26.147767
7×10^{-3}	389607	43.931573	26.154783
4×10^{-3}	389537	43.902165	26.170164

2×10^{-3}	443303	43.867899	26.155349
1.5×10^{-3}	621072	43.698311	26.128872

Note. Own creation.

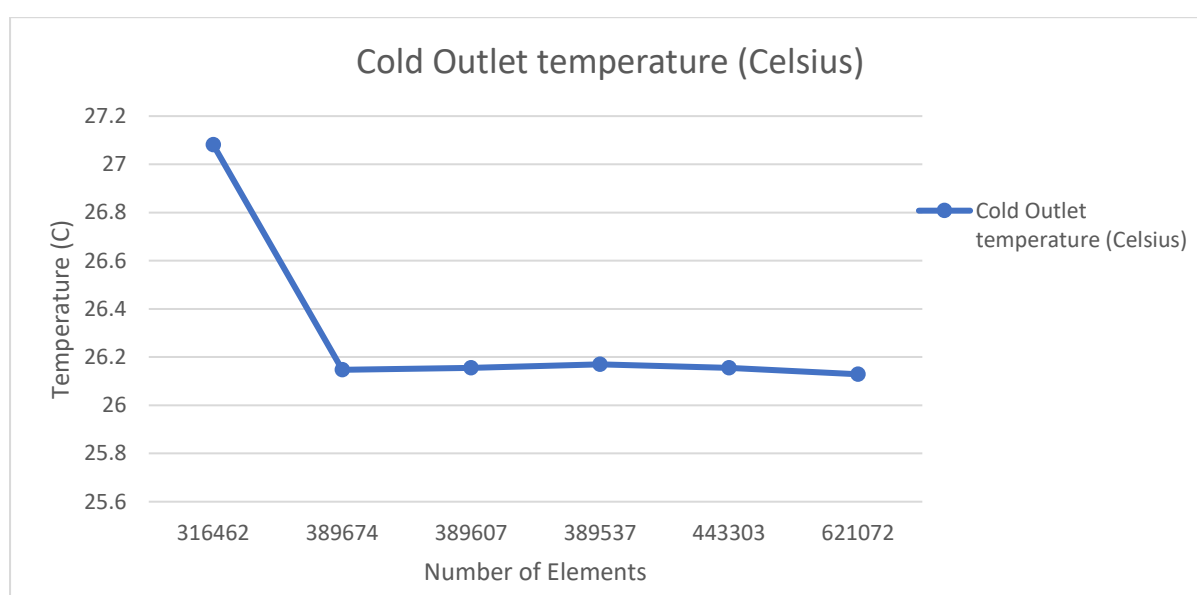
Figures 5 and 6 illustrates the hot and cold outlet temperatures against the element size. Even if the mesh element count has altered in the hot and cold temperature scenarios, the temperatures are still relatively close. It demonstrates that after a certain point, changing the mesh size has no noticeable effect on the temperature and other parameters if the mesh is of good quality. For a study, a poor-quality mesh was used with the element size of 12.4×10^{-2} mm which has considerable effect on the cold outlet temperature.

Figure 5: Hot outlet temperature against number of elements



Note. Own creation.

Figure 6: Cold outlet temperature against number of elements



Note. Own creation.

Results

The following tables 4 and 5 compile the results obtained from the 3D simulations. Similarly, to the 2D simulation covered in coursework 1 experiments 1 and 2 were recreated in the 3D simulation. This was done to obtain results that can be directly compared to the experimental and 2D simulation results. The calculations performed are described in coursework 1.

Experiment 1 featured varying cold flow rates, the results can be found in table 4. Experiment 2 featured constant cold and hot flow rates; the results can be found in table 5.

Expanding on the results from coursework 1 the 3D simulation results were plotted on top of the 2D and experimental results graph. This enables a clear visual representation of the temperatures of both flows in the heat exchanger. The plotted results can be found in figures 7 and 8 for experiment 1 and 2 respectively.

Table 4: 3D simulation results for experiment 1

Hot flow, L/min	Cold flow, L/min	Th1, °C	Th2, °C	ΔT_h , °C	\overline{T}_h , °C	Tc1, °C	Tc2, °C	ΔT_c , °C	\overline{T}_c , °C	η_h , %	η_c , %	ρ_h , kg/m ³	ρ_c , kg/m ³	C_{ph} , J/(kg K)	C_{pc} , J/(kg K)	Q_e , W	Q_a , W	C_{EB}	$\bar{\eta}$, %	LMTD, °C	U, W
0.66	1.61	51.1	42.45	8.65	46.76	20.9	25.09	5.00	23.40	28.64%	13.87%	989.44	997.61	4179.56	4180.18	393.49	559.50	1.42	21.26%	23.71	829.8
0.73	1.41	51.6	43.51	8.09	47.56	20.1	25.61	5.51	22.86	25.68%	17.49%	989.14	997.47	4179.73	4180.54	406.94	539.95	1.33	21.59%	24.68	824.5
0.73	1.19	51.4	44.08	7.32	47.74	21.6	26.09	4.49	23.85	24.56%	15.07%	989.18	997.37	5179.71	4179.76	456.31	371.24	0.81	19.82%	23.87	955.9

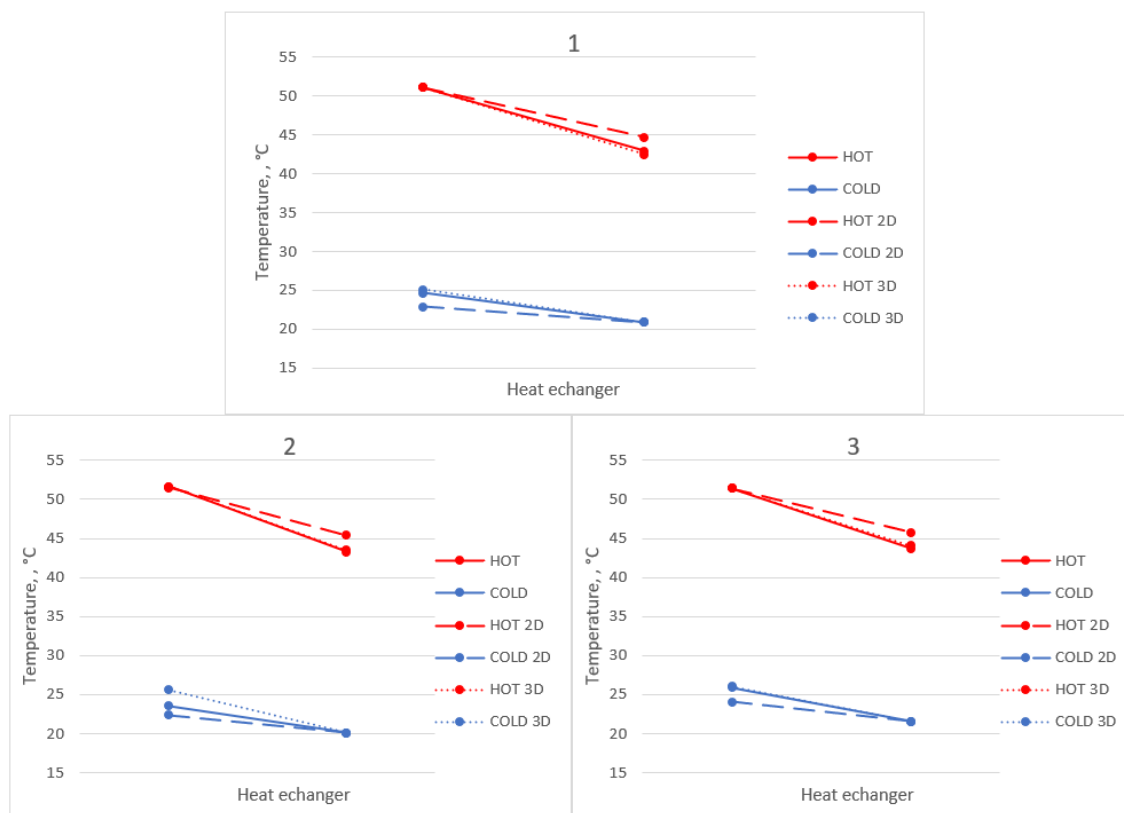
Note. Own creation.

Table 5: 3D simulation results for experiment 2

Hot flow, L/min	Heater temperature, °C	Th1, °C	Th2, °C	ΔT_h , °C	\overline{T}_h , °C	Tc1, °C	Tc2, °C	ΔT_c , °C	\overline{T}_c , °C	η_h , %	η_c , %	ρ_h , kg/m ³	ρ_c , kg/m ³	C_{ph} , J/(kg K)	C_{pc} , J/(kg K)	Q_e , W	Q_a , W	C_{EB}	$\bar{\eta}$, %	LMTD, °C	U, W
0.71	55.6	51.0	43.9	7.1	47.5	21.7	26.17	4.47	23.935	24.23%	15.26%	989.10	997.65	4179.76	4180.26	347.34	369.73	1.06	19.74%	23.49	739.3
0.8	50.2	50.0	42.38	7.6	46.2	19.4	24.29	4.89	21.845	24.90%	15.98%	989.40	997.97	4179.58	4180.95	420.14	540.69	1.29	20.44%	24.32	863.8
0.78	48.1	48.2	40.83	7.4	44.5	19.1	23.95	4.85	21.525	25.33%	16.67%	990.21	998.06	4179.15	4181.17	396.48	536.34	1.35	21.00%	22.97	863.2

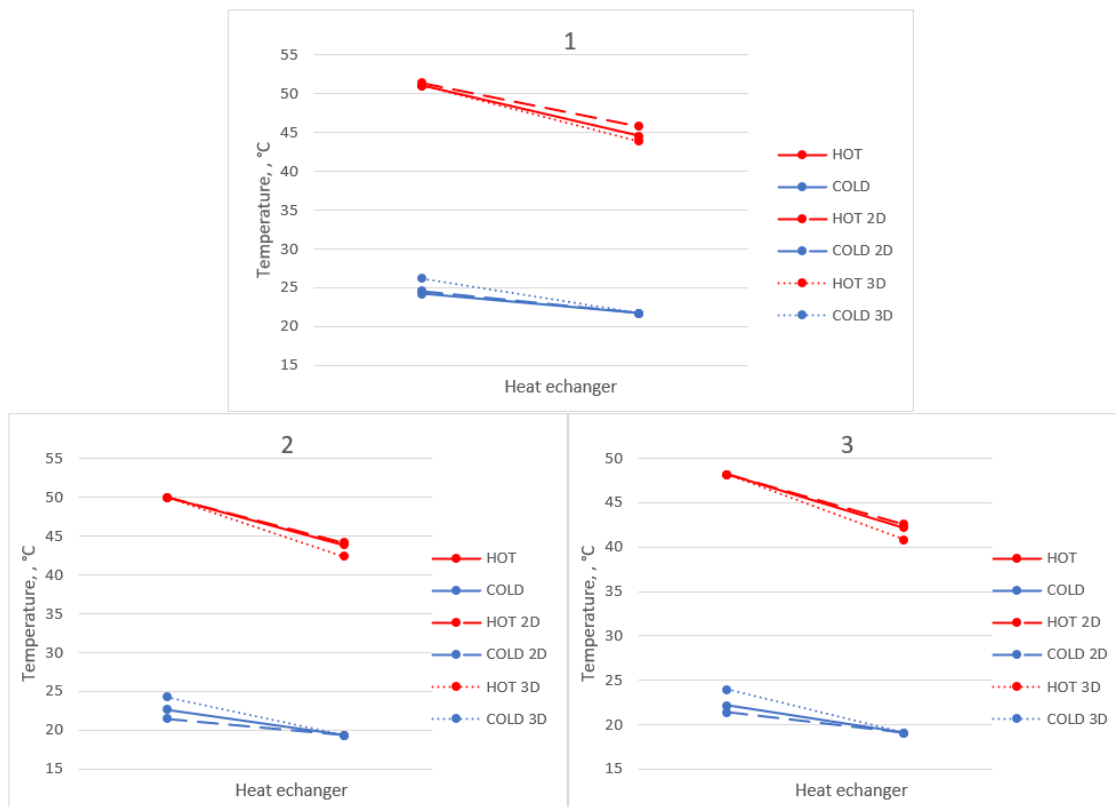
Note. Own creation.

Figure 8: Experimental, 2D and 3D results for experiment 1



Note. Own creation.

Figure 7: Experimental, 2D and 3D results for experiment 2

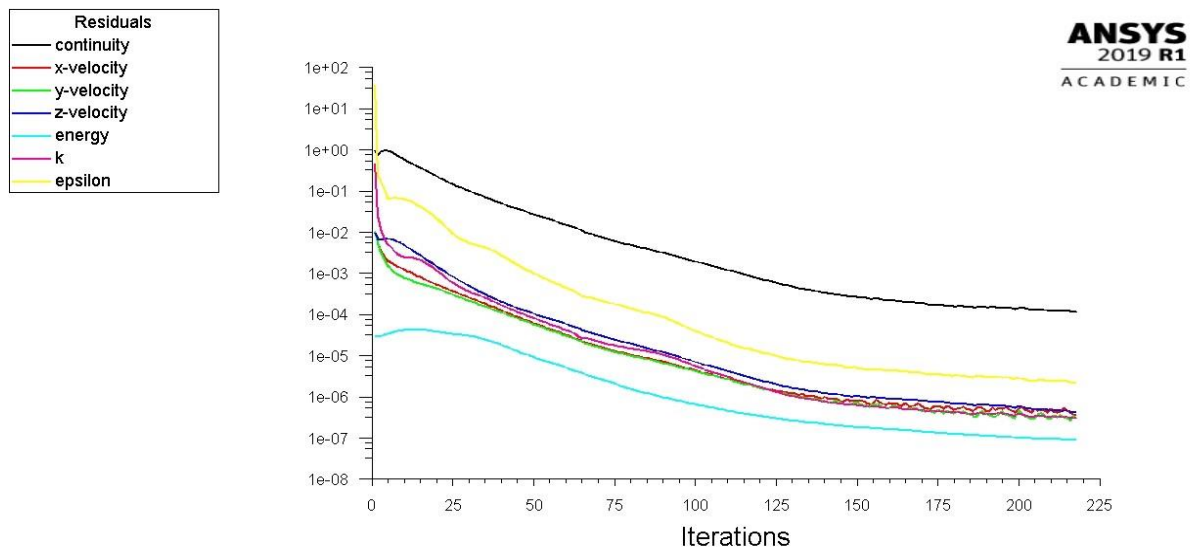


Note. Own creation.

Convergence criteria

Most of the residuals are below the order of magnitude 1×10^{-6} and satisfy the convergence criteria (Kuron, 2015), but the continuity residuals do not reduce to three orders of magnitude as can be seen in figure 9. Although the solution was stabilised, the simulation may not have fully converged. The residuals appear to decrease as the iterations continue. Since prolonged simulation runs may result in a more accurate solution and the convergence criteria. The residual convergence graph for different temperature experiments and the flow rate experiments can be found in the appendix.

Figure 9: Residual convergence graph of a 3D model at a heater temperature of 56.7 °C

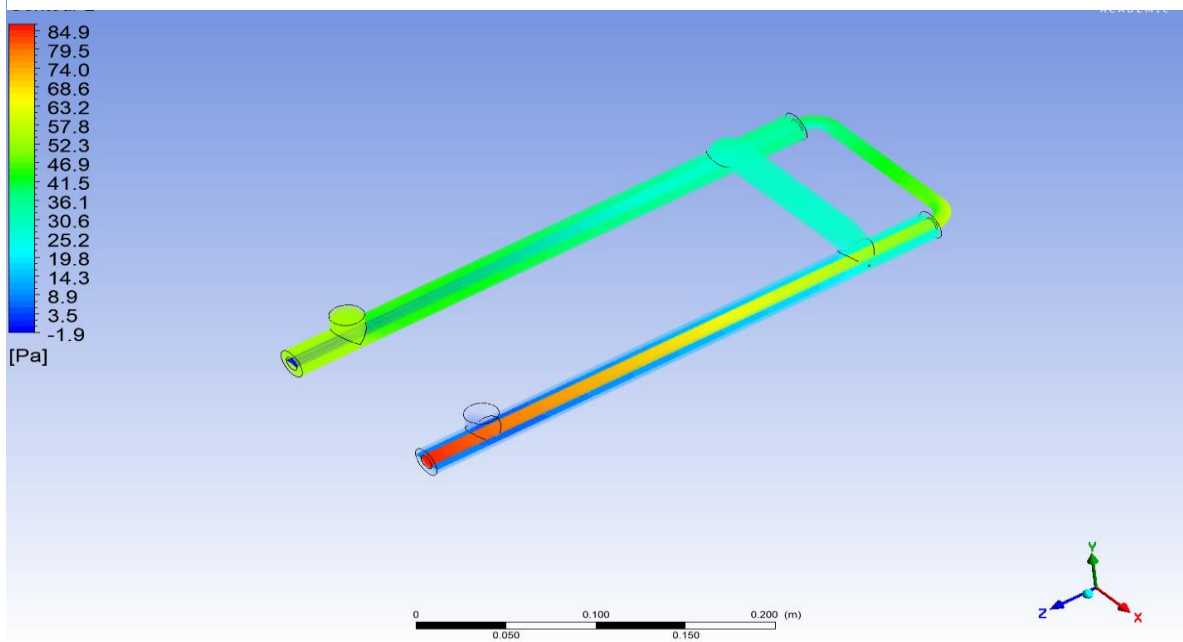


Note. Own creation.

Pressure gradient

Figure 10 illustrates the pressure gradient throughout the heat exchanger in an isometric. At each end on the heat exchanger, the pressure is the highest, and as it moves toward the outlet, it progressively reduces. Due to high velocity in the inner tube the pressure in the inner tube inlet is higher in comparison to the outer inlet. The maximum pressure at the inner tube inlet and the inner outlet has the value of 84.9 Pa and 3.5 Pa respectively. Similarly, the maximum pressure is 57.8 Pa at the outer tube inlet and 8.9 Pa at the outer outlet. Both 2D and 3D models show a similar pressure gradient, the 3D model however, forecasts pressure of a higher magnitude in comparison to 2D. It is expected that the 3D simulation depicts a more accurate pressure gradient due to the complex geometry of a 3D model.

Figure 10: Isometric view of the change in pressure

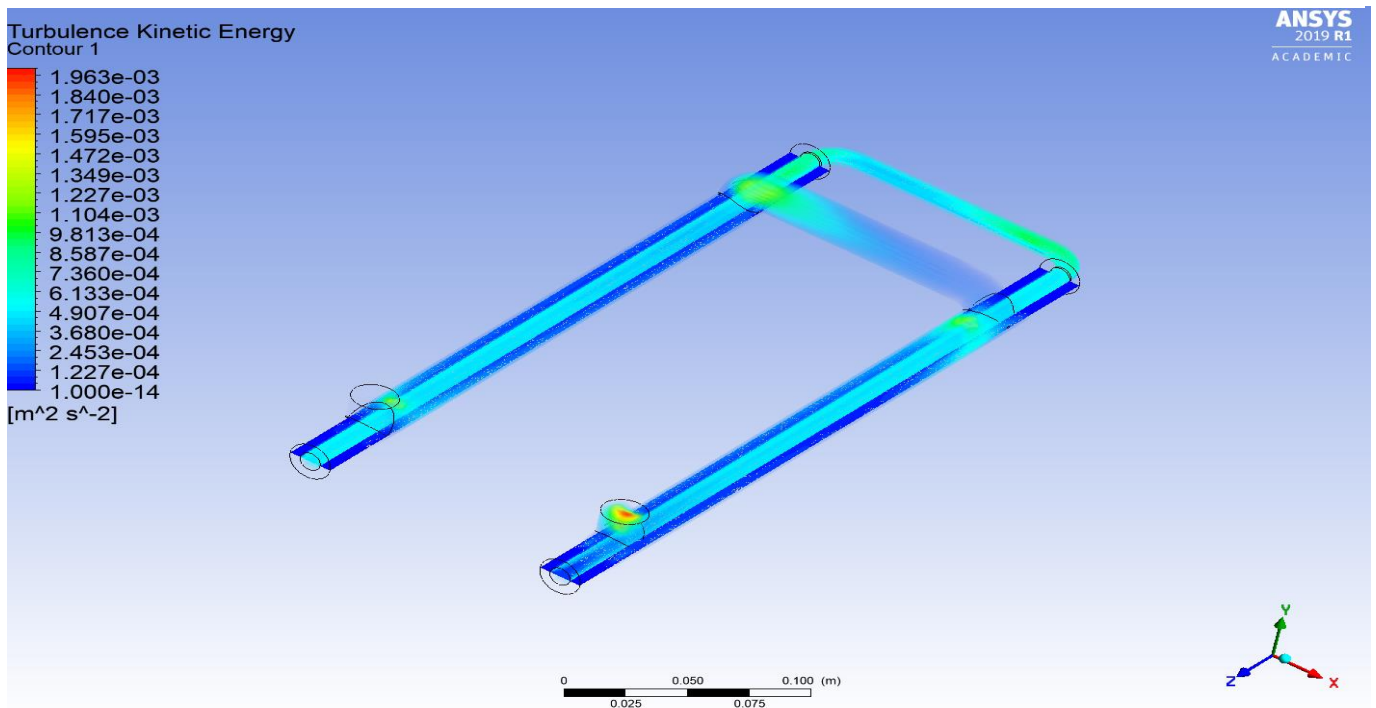


Note. Own creation.

Velocity profile

Figure 11 provides a 3D illustration of the velocity across the heat exchanger. The velocity is inversely proportional with the pressure. Therefore, the velocity in the inlets of each pipe is lower than the outlets which can be clearly seen in the figure 11. However, only slight increase in the velocity can be observed as the flow moves forward. The velocity in the inner tube inlet is 0.1 m/s and at the inner tube outlet is 0.2 m/s whereas the outer pipe inlet has a velocity slightly higher than 0 m/s and an outlet velocity of 0.1 m/s. The no-slip boundary condition is demonstrated by the fact that, the velocity on the wall is zero, indicating that there is no fluid moment across the walls. The velocity demonstration in the 3D model is more accurate in comparison to the 2D model. In the 2D model, the velocity of the outer tube appears to be almost constant throughout the pipe, while the 3D depiction shows a slight variation in velocity.

Figure 12: Turbulence profile

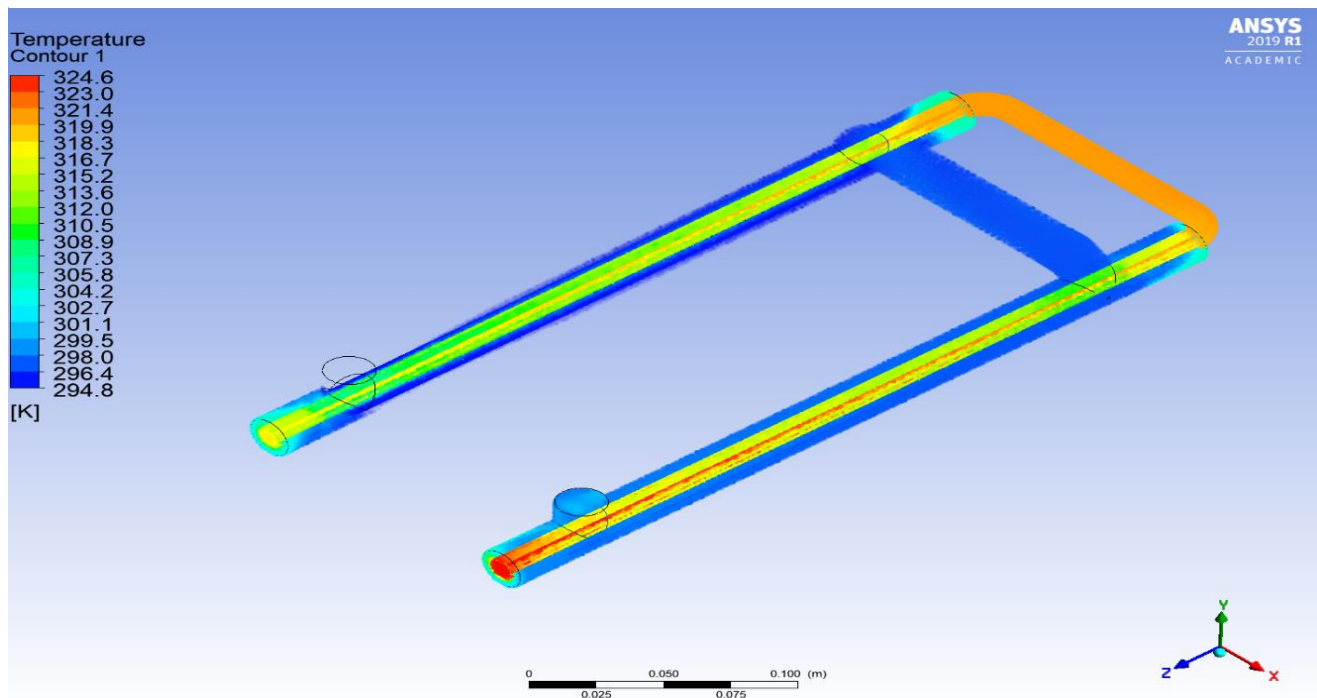


Note. Own creation

Temperature profile

Figure 17 represents the temperature gradient throughout the heat exchanger in an isometric view. The temperature of the fluid in the outer tube progressively rises, reaching a maximum temperature of 299.5 K at the outlet. Similarly, conduction between the hot fluid in the inner pipe and the cold fluid in the outer pipe causes the temperature of the hot fluid to drop, finally reaching the outlet temperature of almost 318.7 K. The fluids temperature at the convection zone in the inner pipe is slightly higher than the mid-zone of each pipe. The 3D model is important to display the detail perspective of temperature in the overall heat exchanger even if the output temperature results from 2D and 3D are fairly similar. For instance, convection temperature is not accounted for in the 2D model.

Figure 13: Temperature profile



Note. Own creation.

Discussion

The 3D simulation created using ANSYS 2019 was successful at producing usable and consistent results. The results for both 2D and 3D simulations can vary due to factors such as the design of the model or mesh convergence. Therefore, it is important to develop the most accurate design to obtain the most accurate results. Compared to experimental results and 2D simulation results the 3D simulation featured the highest performance of the heat exchanger. The mean efficiencies and heat transfer coefficients gathered from the 3D results are higher than the experimental and 2D results. This is to be expected compared to experimental results as the simulation was not made to account for minor heat losses and did not account for errors, the difference between the 2D results is unclear and might be an indication of a problem with the 2D model. For experiment 1 the 3D simulation produced results very close to the experimental results, especially for the hot flow temperatures, where the largest difference was 0.5 °C, however, the cold-water outlet temperatures had a larger difference in temperatures. 3D results for experiment 2 featured a larger discrepancy and were further away from the experimental results compared to the 2D results. This can be attributed to many reasons such as unstable flow conditions in the experiment or imperfections in the 3D model, however, more tests must be performed to reach a conclusion. The graphs comparing 2D, 3D, and experimental results clearly depict the case that the difference between the 3D results and experimental results fluctuate, in some cases the 3D simulation produced almost identical results, however in other cases there is a noticeable difference. This can again be attributed to unstable flow conditions in the experiment, errors in the experimental results, or inaccuracies in the 3D model.

Table 3 demonstrates that the outcomes are influenced by poor-quality meshes with larger element sizes, whereas good meshes, after a certain point, are unaffected by changes in the element size. The quality of the mesh was improved using different meshing techniques such as automatic mesh, edge sizing, tetrahedral geometry along with an improvement in skewness, orthogonal quality and the aspect ratio of the mesh. However, the inflation mesh was not used due to a warning that popped up mentioning the stairsteps has been created at some location of mesh due to inflation. For more clear

observation of influence of mesh on the results, some worst quality mesh could be used, and the generated data would be compared to the excellent mesh. However, the results were compared with the good and slightly bad quality mesh. With the proper research of inflation mesh utilization, it could be deployed in the mesh which could create a finer mesh near the walls, producing more accurate results. Similarly, to be certain of convergence, wall shear stress as well as inlet-pressure plot could be created which provides information on whether the boundary layer has stabilized and provides a good indication of the pressure drop across the wall respectively.

As discussed in coursework 1, element size influences the simulation time, the larger element size, the less time consuming and the vice versa. Therefore, it is important to keep this in mind while running time-consuming simulations.

The pressure gradient in 2D and 3D shows the gradients along the heat exchanger and the crucial areas estimated by both 2D, and 3D models were similar. However, in contrast to 2D, the 3D model predicts pressure of a greater magnitude. Hence, 2D modelling is adequate for rapid simulations or for obtaining quick results, but 3D modelling should be done if precise values are needed.

Conclusion

A 3D model was successfully created, and usable data was gathered and compared with the results from the 2D simulation and the experiment. This report has expanded on the findings of coursework 1 and proven the 3D model to be a better solution for identifying and visualizing turbulence, temperature, and pressure profiles. Both 2D and 3D models have viable applications, as the 3D simulation can take much longer to complete especially if solving a more complicated problem. Depending on the complexity of the problem 2D and 3D models can both provide very accurate results, however 2D simulations are generally more limited. CFD simulations are mathematical models dependent on inputs, which is why to obtain the most accurate results the simulations must be run with accurate inputs simulating the real-life problem as well as the geometry and mesh of the model has to be carefully constructed to best fit the application.

The findings from coursework 1 and 2 conclude that both 2D and 3D CFD simulations provide viable solutions to real life problems and the accuracy of the results is dependent on the quality of the model.

Bibliography

ANSYS. (2009, January 29). *6.2.2 Mesh Quality*. Retrieved from ANSYS .

ANSYS. (2009, January 29). *ANSYS FLUENT 12.0 User's Guide*. Retrieved from ANSYS:
<https://www.afs.enea.it/project/neptunius/docs/fluent/html/ug/node1.htm>

Kuron, M. (2015). *Criteria for Assessing CFD Convergence | Engineering.com*.
<https://www.engineering.com/story/3-criteria-for-assessing-cfd-convergence>

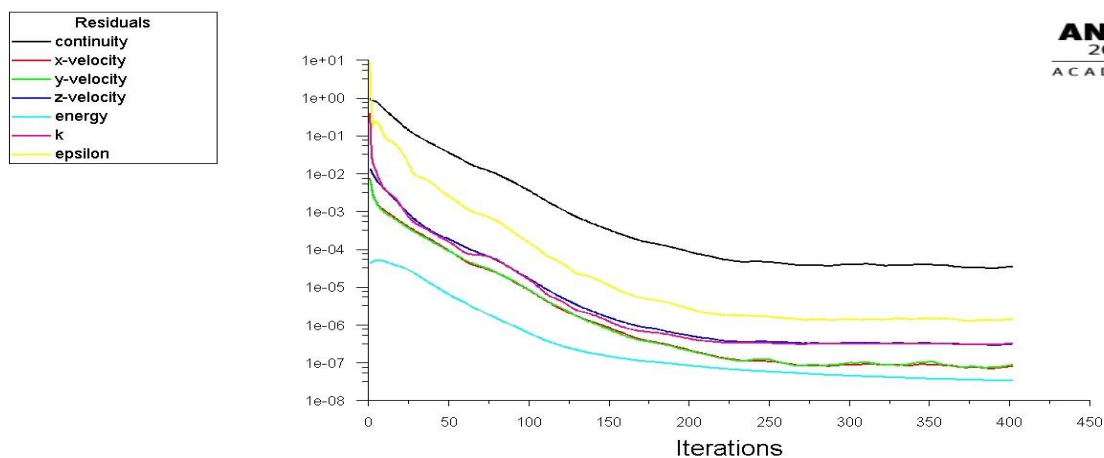
Leap CFD team. (2011). *Tips & Tricks: Size Controls in ANSYS | Computational Fluid Dynamics (CFD) Blog – LEAP Australia & New Zealand*. <https://www.computationalfluiddynamics.com.au/size-controls/>

Qubeissi, M. (2022). *CW2 brief*.
<https://coventry.aula.education/?#/dashboard/b1d9645d-de7a-4c7d-9ad3-2d0c17295179/journey/materials/de79dab3-9e52-4704-997a-85196ddf2b2a>

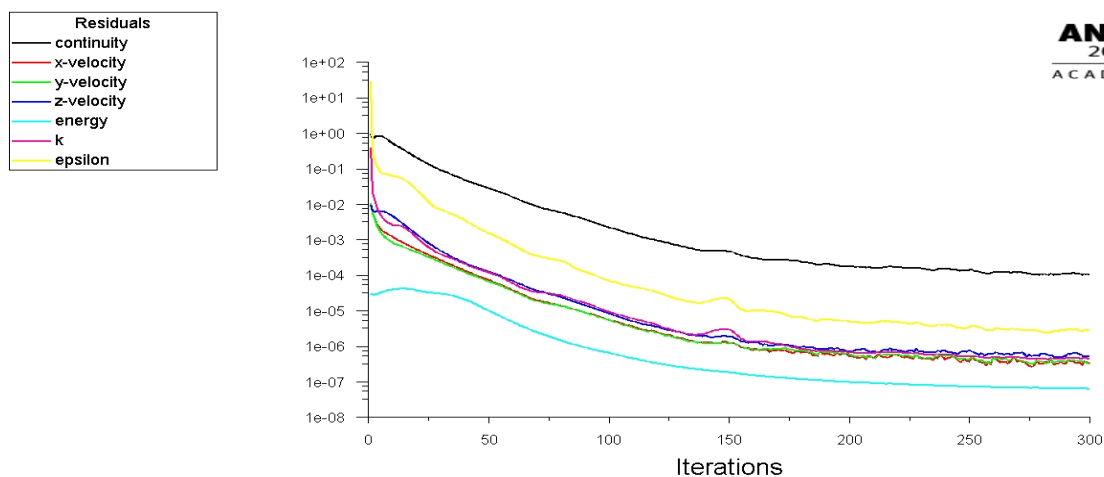
Simscale. (n.d.). *K-epsilon Turbulence Model | Global Settings | SimScale*. Retrieved November 10, 2022, from <https://www.simscale.com/docs/simulation-setup/global-settings/k-epsilon/>

Appendix

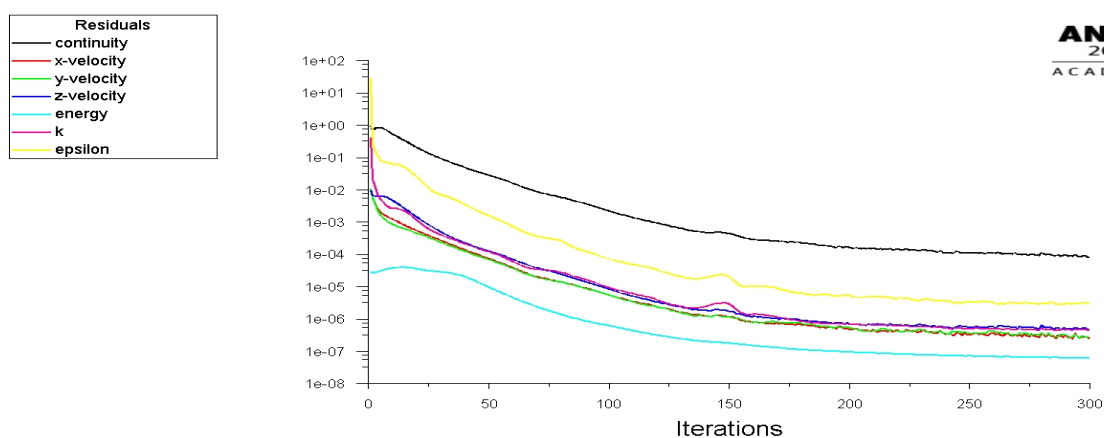
Appendix A. Residual convergence graph of a 3D model with bad mesh quality.



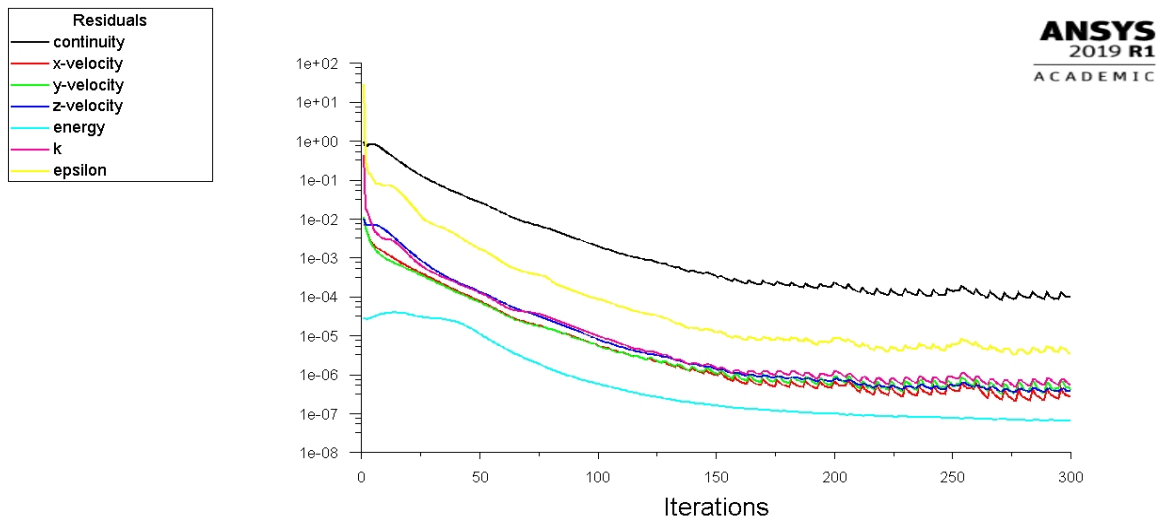
Appendix B. Residual convergence graph of a 3D model for a heater temperature of 50.2°C.



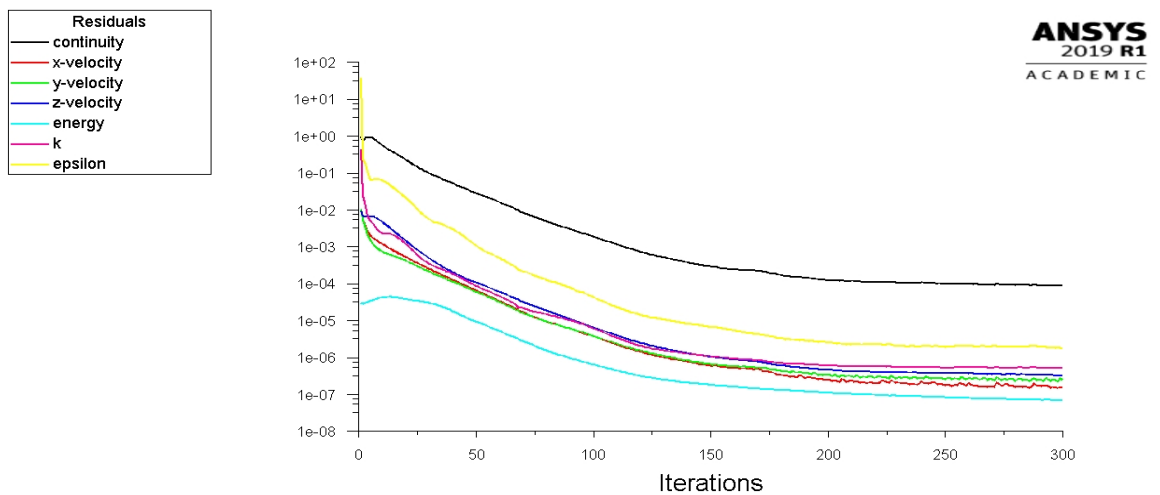
Appendix C. Residual convergence graph of a 3D model for a heater temperature of 48.1°C.



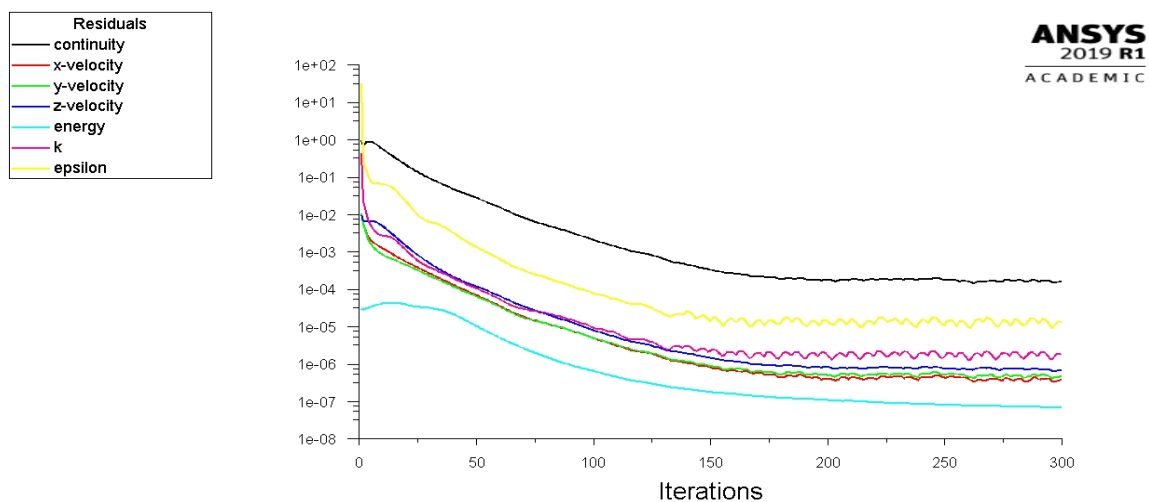
Appendix D. Residual convergence graph of a 3D model with a hot flowrate of 0.66 L/min and a cold flowrate of 1.61 L/min.



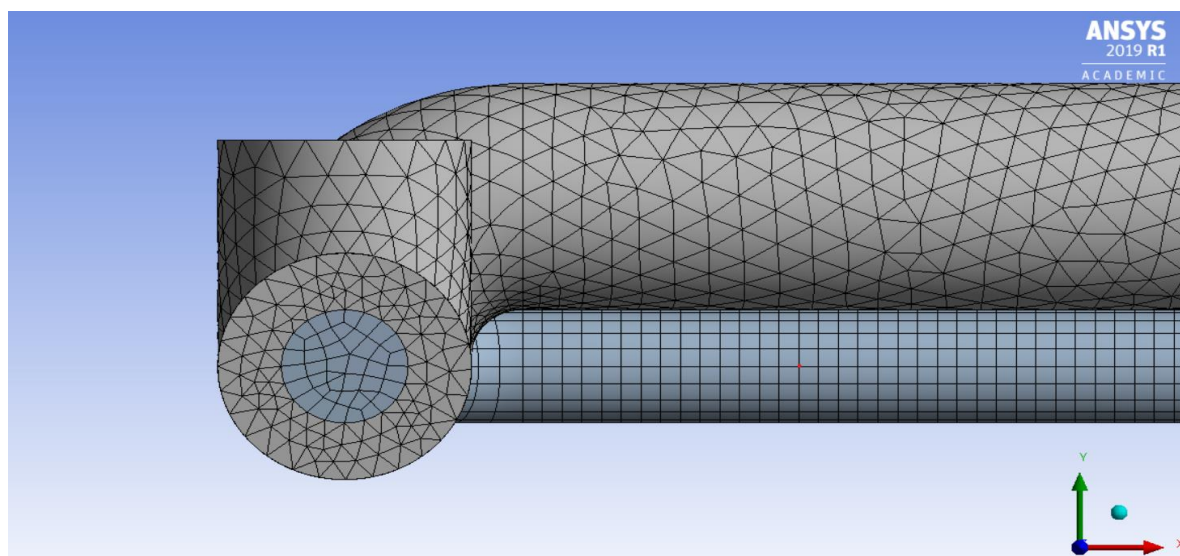
Appendix E. Residual convergence graph of a 3D model with a hot flowrate of 0.73 L/min and a cold flowrate of 1.19L/min.



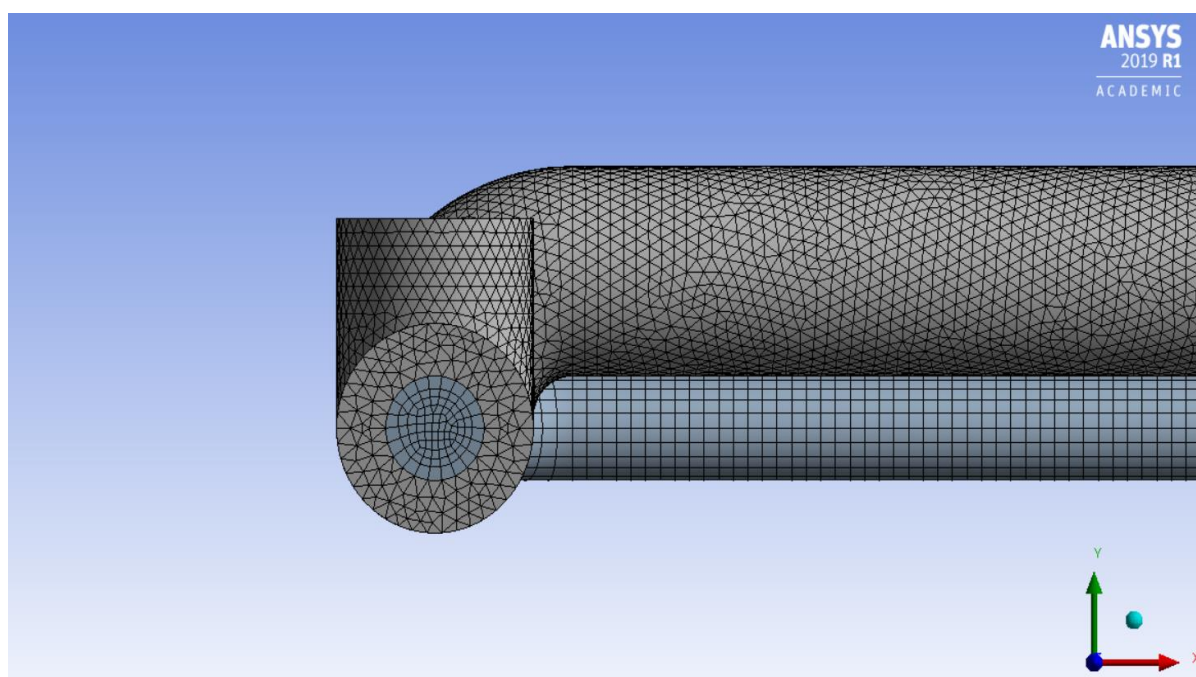
Appendix F. Residual convergence graph of a 3D model with a hot flowrate of 0.73 L/min and a cold flowrate of 1.41L/min.



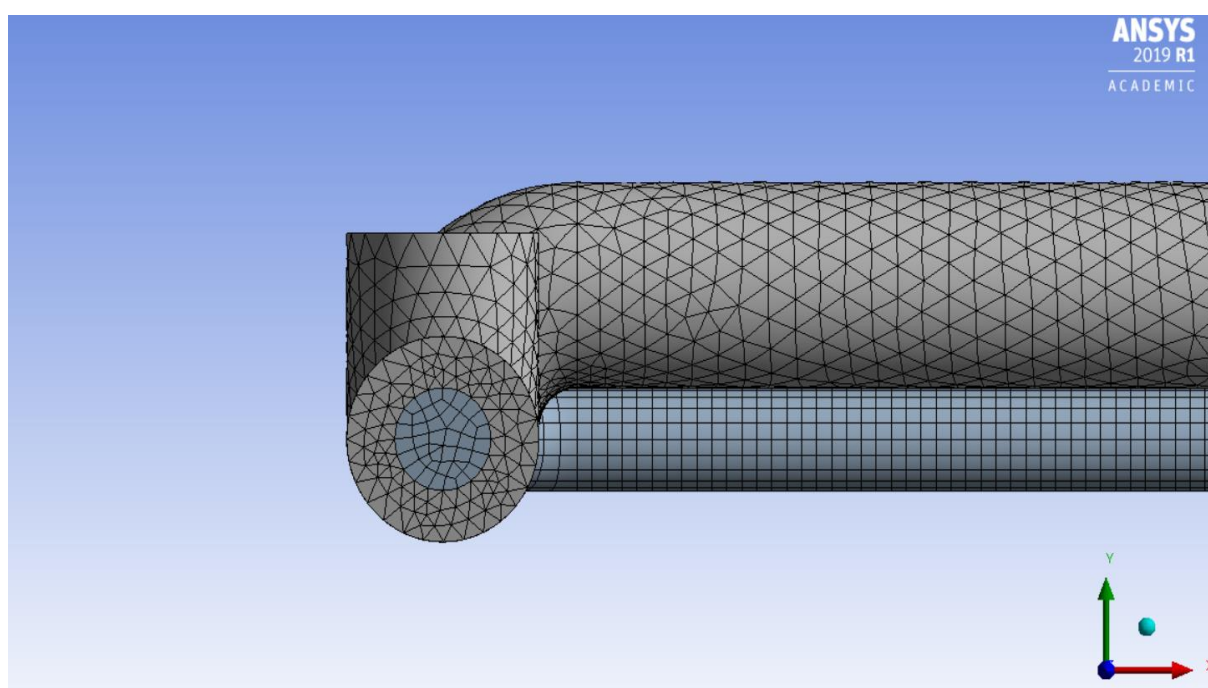
Appendix G. 3D model mesh with an element size of 12.4×10^{-2} m.



Appendix H. 3D model mesh with an element size of 1.5×10^{-3} m.



Appendix I. 3D model mesh with an element size of 10×10^{-3} m.



Appendix J. mass flow inlet and hydraulic for outer pipe.

F

Mass-Flow Inlet

×

Zone Name

cold_inlet

Momentum

Thermal

Radiation

Species

DPM

Multiphase

Potential

UDS

Reference Frame

Absolute

Mass Flow Specification Method

Mass Flow Rate

Mass Flow Rate (kg/s)

0.0198

Supersonic/Initial Gauge Pressure (pascal)

0

Direction Specification Method

Normal to Boundary

Turbulence

Specification Method

Intensity and Hydraulic Diameter

Turbulent Intensity (%)

5

Hydraulic Diameter (mm)

8

OK

Cancel

Help

Appendix K. Mass flow inlet and hydraulic diameter for inner pipe.

F

Mass-Flow Inlet

×

Zone Name

hot_inlet

Momentum

Thermal

Radiation

Species

DPM

Multiphase

Potential

UDS

Reference Frame

Absolute

Mass Flow Specification Method

Mass Flow Rate

Mass Flow Rate (kg/s)

0.0117

Supersonic/Initial Gauge Pressure (pascal)

0

Direction Specification Method

Normal to Boundary

Turbulence

Specification Method

Intensity and Hydraulic Diameter

Turbulent Intensity (%)

5

Hydraulic Diameter (mm)

10

OK

Cancel

Help

Appendix L. wall thickness and the material used for the conduction pipe (inner pipe).

Wall

×

Zone Name

inner_pipe

Adjacent Cell Zone

cold_domain

Shadow Face Zone

inner_pipe-shadow

Momentum

Thermal

Radiation

Species

DPM

Multiphase

UDS

Wall Film

Potential

Structure

Thermal Conditions

Heat Flux

Temperature

Coupled

Wall Thickness (mm)

1

Heat Generation Rate (w/m3)

0

Shell Conduction

1 Layer

Edit...

Material Name

steel

Edit...

Appendix M. Heat flux and material used for the insulation wall (Outer pipe outer surface).

Wall

×

Zone Name

insulation_wall

Adjacent Cell Zone

cold_domain

Momentum

Thermal

Radiation

Species

DPM

Multiphase

UDS

Wall Film

Potential

Structure

Thermal Conditions

Heat Flux

Temperature

Convection

Radiation

Mixed

via System Coupling

via Mapped Interface

Heat Flux (w/m2)

0

Wall Thickness (mm)

0

Heat Generation Rate (w/m3)

0

Shell Conduction

1 Layer

Edit...

Material Name

acrylic

Edit...

OK

Cancel

Help